Available online at www.sciencedirect.com
ScienceDirect
Advances in Space Research 43 (2009) 1940–1944
ADVANCES IN SPACE RESEARCH (a COSPAR publication)
www.elsevier.com/locate/asr

Broadband electrostatic noise and low-frequency waves in the Earth's magnetosphere

S.V. Singh *, R.V. Reddy, G.S. Lakhina

Indian Institute of Geomagnetism, New Panvel (West), Navi, Mumbai-410 218, India

Received 9 January 2007; received in revised form 23 February 2009; accepted 25 February 2009

Abstract

Broadband electrostatic noise (BEN) is commonly observed in different regions of the Earth's magnetosphere, eg., auroral region, plasma sheet boundary layer, etc. The frequency of these BENs lies in the range from lower hybrid to the local electron plasma frequency and sometimes even higher. Spacecraft observations suggest that the high and low-frequency parts of BEN appear to be two different wave modes. There is a well established theory for the high-frequency part which can be explained by electrostatic solitary waves, however, low-frequency part is yet to be fully understood. The linear theory of low-frequency waves is developed in a four-component magnetized plasma consisting of three types of electrons, namely cold background electron, warm electrons, warm electron beam and ions. The electrostatic dispersion relation is solved, both analytically and numerically. For the parameters relevant to the auroral region, our analysis predict excitation of electron acoustic waves in the frequency range of 17 Hz to 2.6 kHz with transverse wavelengths in range of (1–70) km. The results from this model may be applied to explain some features of the low-frequency part of the broadband electrostatic noise observed in other regions of the magnetosphere.

Keywords: Broadband electrostatic noise; Low-frequency waves; Magnetosphere

1. Introduction

Satellite observations in different regions of the Earth's magnetosphere have shown the existence of broadband electrostatic noise (BEN) emissions with frequencies from ion plasma and lower hybrid frequencies up to and higher than the electron plasma and cyclotron frequencies. However, most of the power is concentrated in the vicinity of ion plasma and lower hybrid frequencies. In the plasma sheet boundary layer (PSBL), the frequency range of BEN spans from $\sim$10 Hz up to $\sim$10 kHz and beyond. The high time resolution data analysis have shown that BEN consists of small scale, large amplitude, magnetic field aligned electric fields in the auroral acceleration region (Temerin et al., 1982; Bostrom et al., 1988; Mozer et al., 1997; Ergun et al., 1998; Bounds et al., 1999; Pottelette et al., 1999), in the plasma sheet boundary layer (PSBL) (Matsumoto et al., 1994), in the Earth's high altitude polar magnetosphere (Franz et al., 1998), in polar cap boundary layer (PCBL) (Tsurutani et al., 1998), and on cusp field lines (Cattell et al., 1999). These spiky structures in the parallel electric field are interpreted as solitons (Temerin et al., 1982) or phase space holes (Omura et al., 1994). The scale sizes and electric field amplitude of these structures can range from 100 to 1000 m and few 10s to few 100s mV/m, respectively. BENs are observed in conjunction with the ion and electron beams. The high-frequency component of BEN can be explained in terms of electrostatic impulsive solitary waves (Matsumoto et al., 1994; Omura et al., 1994). But low-frequency part of the BEN has not been understood properly.

Several linear theories based on electron-acoustic instabilities (Tokar and Gary, 1984; Gary and Tokar, 1985; Bharuthram, 1991; Singh and Lakhina, 2001; Sooklal and

* Corresponding author. Tel.: +91 22 27484149; fax: +91 22 27480762.
E-mail address: satyavir@iigs.iigm.res.in (S.V. Singh).

0273-1177/$36.00 © 2009 COSPAR. Published by Elsevier Ltd. All rights reserved.
doi:10.1016/j.asr.2009.02.015

Mace, 2004) have been developed in order to explain the higher frequency part of BEN spectrum. However, still there is no satisfactory explanation for low-frequency part of the BEN. Tokar and Gary (1984) analyzed the full electromagnetic Vlasov dispersion equation and studied the stability of the electrostatic and electromagnetic waves for the case of upward moving electron beams observed in the polar cusp region. Their numerical simulations showed electron-acoustic waves (EAWs) to be unstable. Singh and Lakhina (2001) studied the generation of electron-acoustic waves (EAWs) in an unmagnetized, four-component plasma consisting of stationary cold and hot Maxwellian electrons, drifting electron beam and ions. The addition of hot background electrons to the previously existing three-component models reduces the excited EAW frequencies and growth rates. Electron-acoustic instability in a magnetized three electron component plasma driven by field aligned electron beam has been studied by Sooklal and Mace (2004). They discussed electron-acoustic waves in the limits of weakly as well as strongly magnetized plasma. In this paper, low frequency waves ($\omega << \omega_{ce}$) are studied in a magnetized plasma consisting of cold, hot and beam electrons and ions. The model is applied to explain some features of the low-frequency component of the broadband electrostatic noise (BEN) observed in the Earth's magnetosphere.

2. Dispersion relation

We consider a homogeneous plasma with four components, cold background electrons, drifting warm beam electrons, hot electrons and ions. Electrons are magnetized and ions are considered unmagnetized. The dispersion relation for the electrostatic waves in such a plasma can be written as (Roth and Hudson, 1986)

$$1+\sum_{l=-\infty}^{\infty}\frac{\omega_{pc}^2 I_l e^{-\lambda_c}}{k^2 v_{tc}^2}\left[1+\frac{\omega}{\sqrt{2}k_\parallel v_{tc}}Z(\xi_c)\right] +\sum_{l=-\infty}^{\infty}\frac{\omega_{ph}^2 I_l e^{-\lambda_h}}{k^2 v_{th}^2}\left[1+\frac{\omega}{\sqrt{2}k_\parallel v_{th}}Z(\xi_h)\right] +\sum_{l=-\infty}^{\infty}\frac{\omega_{pb}^2 I_l e^{-\lambda_b}}{k^2 v_{tb}^2}\left[1+\frac{\omega-k_\parallel U_b}{\sqrt{2}k_\parallel v_{tb}}Z(\xi_b)\right] +\frac{\omega_{pi}^2}{k^2 v_{ti}^2}\left[1+\frac{\omega}{\sqrt{2}kv_{ti}}Z(\xi_i)\right]=0, \tag{1}$$

where $\xi_i=\frac{\omega}{\sqrt{2}kv_{ti}}, \xi_{c,h}=\frac{\omega-l\omega_{ce}}{\sqrt{2}k_\parallel v_{tc,h}}$ and $\xi_b=\frac{\omega-k_\parallel U_b-l\omega_{ce}}{\sqrt{2}k_\parallel v_{tb}}$, $\lambda_j=k_\perp^2 v_{tj}^2/\omega_{ce}^2$, where $j = c$, h, b stands for cold, hot and beam electrons, respectively.

Z is the plasma dispersion function with respect to its argument, $v_{tj}=\sqrt{T_j/m_j}$ is the thermal speed of the jth species; T_j and m_j are temperature and mass of the jth species; $\lambda_{dj}=v_{tj}/\omega_{pj}$ (ω_{pj} is the plasma frequency) is the Debye length of the jth species and ω and k represents the frequency and wave number, respectively, and U_b is the electron beam drift speed.

To simplify the dispersion relation (1), we assume ions as unmagnetized and cold, i.e., $\omega >> \sqrt{2}kv_{ti}$; for hot electrons, we consider $(\omega - l\omega_{ce}) >> \sqrt{2}k_\parallel v_{th}$ for all values of l except $l = 0$ for which $\omega \leqslant \sqrt{2}k_\parallel v_{th}$; for cold electrons, we take $(\omega - l\omega_{ce}) >> \sqrt{2}k_\parallel v_{tc}$ for all l, and for resonant warm beam electrons, we consider $(\omega - l\omega_{ce} - k_\parallel U_b) \leqslant \sqrt{2}k_\parallel v_{tb}$. Then, on expanding the various plasma dispersion function according to the above approximations on their arguments, we obtain the following simplified dispersion relation in a four-component plasma,

$$1-\frac{\omega_{pi}^2}{\omega^2}+\sum_{l=-\infty}^{\infty}\frac{\omega_{pc}^2 I_l e^{-\lambda_c}}{k^2 v_{tc}^2}\left[1-\frac{\omega}{\omega-l\omega_{ce}}-\frac{\omega k_\parallel^2 v_{tc}^2}{(\omega-l\omega_{ce})^3}+i\sqrt{\frac{\pi}{2}}\frac{\omega}{k_\parallel v_{tc}}e^{-\xi_c^2}\right] +\frac{\omega_{ph}^2 I_0 e^{-\lambda_h}}{k^2 v_{th}^2}+i\sqrt{\frac{\pi}{2}}\frac{\omega\omega_{ph}^2 I_0 e^{-\lambda_h}}{k_\parallel k^2 v_{th}^3}e^{-\xi_{h0}^2} +\sum_{l\neq 0,l=-\infty}^{\infty}\frac{\omega_{ph}^2 I_l e^{-\lambda_h}}{k^2 v_{th}^2}\left[1-\frac{\omega}{\omega-l\omega_{ce}}-\frac{\omega k_\parallel^2 v_{th}^2}{(\omega-l\omega_{ce})^3}+i\sqrt{\frac{\pi}{2}}\frac{\omega}{k_\parallel v_{th}}e^{-\xi_h^2}\right] +\sum_{l=-\infty}^{\infty}\frac{\omega_{pb}^2 I_l e^{-\lambda_b}}{k^2 v_{tb}^2}\left[1+i\sqrt{\frac{\pi}{2}}\left(\frac{\omega-k_\parallel U_b}{k_\parallel v_{tb}}\right)e^{-\xi_b^2}\right]=0. \tag{2}$$

where $\xi_{h0}=\frac{\omega}{\sqrt{2}k_\parallel v_{th}}$. We have neglected the real part contribution in the expansion of Plasma dispersion function for the warm beam electrons. Considering low-frequency waves $\omega << \omega_{ce}$, we obtain the following dispersion relation

$$1-\frac{\omega_{pi}^2}{\omega^2}-\frac{k_\parallel^2}{k^2}\frac{\omega_{pc}^2}{\omega^2}+\frac{k_\perp^2}{k^2}\frac{\omega_{pc}^2}{\omega_{ce}^2}+\frac{\omega_{ph}^2}{k^2 v_{th}^2}+\frac{\omega_{pb}^2}{k^2 v_{tb}^2} +i\sqrt{\frac{\pi}{2}}\left[\frac{\omega\omega_{ph}^2 I_0(\lambda_h)e^{-\lambda_h}}{k_\parallel k^2 v_{th}^3}e^{-\xi_{h0}^2} +\left(\frac{\omega-k_\parallel U_b}{k_\parallel k^2 v_{tb}^3}\right)\omega_{pb}^2 I_0(\lambda_b)e^{-\lambda_b}e^{-\xi_{b0}^2}\right]=0 \tag{3}$$

where $\xi_{b0}=\frac{\omega-k_\parallel U_b}{\sqrt{2}k_\parallel v_{tb}}$. In the above, we have taken $\lambda_c << 1$, and retained only $l = 0$ terms in the imaginary part because of the low-frequency wave ($\omega << \omega_{ce}$) assumption. The dispersion relations (3) can be further simplified to

$$1-\frac{\omega_{pi}^2}{\omega^2}-\frac{k_\parallel^2}{k^2}\frac{\omega_{pc}^2}{\omega^2}+\frac{k_\perp^2}{k^2}\frac{\omega_{pc}^2}{\omega_{ce}^2}+\frac{1}{k^2\lambda_{dh}^2}+\frac{1}{k^2\lambda_{db}^2} +i\sqrt{\frac{\pi}{2}}\left[\frac{\omega\omega_{ph}^2 I_0 e^{-\lambda_h}}{k_\parallel k^2 v_{th}^3}e^{-\xi_{h0}^2}+\frac{(\omega-k_\parallel U_b)}{k_\parallel k^2 v_{tb}^3}\omega_{pb}^2 I_0 e^{-\lambda_b}e^{-\xi_{b0}^2}\right]=0 \tag{4}$$

Further, substituting for $\omega = \omega_r + i\gamma$; $\gamma << \omega_r$ and separating real and imaginary parts we obtain, the following expressions for real frequency and growth rate, respectively. The real frequency of the wave can be given by

$$\omega_r = \frac{\omega_{pi}\sqrt{1+\frac{k_\parallel^2}{k^2}\frac{m_i}{m_e}\frac{n_c}{n_i}}}{\sqrt{1+\frac{k_\perp^2}{k^2}\frac{\omega_{pc}^2}{\omega_{ce}^2}+\frac{1}{k^2\lambda_{dh}^2}+\frac{1}{k^2\lambda_{db}^2}}} \quad (5)$$

and the growth rate can be written as

$$\frac{\gamma}{\omega_r} = -\sqrt{\frac{\pi}{8}}\frac{\left[\frac{\omega_r\omega_{ph}^2 I_0(\lambda_h)e^{-\lambda_h}}{k_\parallel k^2 v_{th}^3}e^{-\xi_{h0}^2}+\frac{(\omega_r-k_\parallel U_b)\omega_{pb}^2 I_0(\lambda_b)e^{-\lambda_b}}{k_\parallel k^2 v_{tb}^3}e^{-\xi_{b0}^2}\right]}{1+\frac{k_\perp^2}{k^2}\frac{\omega_{pc}^2}{\omega_{ce}^2}+\frac{1}{k^2\lambda_{dh}^2}+\frac{1}{k^2\lambda_{db}^2}}. \quad (6)$$

The condition for the growth of the wave is that the beam speed should exceed a critical value u_{cr}, i.e., be

$$U_b > u_{cr} = \frac{\omega_r}{k_\parallel}\left[1+\frac{n_h}{n_b}\left(\frac{T_b}{T_h}\right)^{3/2}\frac{I_0(\lambda_h)e^{-\lambda_h}e^{-\xi_{h0}^2}}{I_0(\lambda_b)e^{-\lambda_b}e^{-\xi_{b0}^2}}\right] \quad (7)$$

3. Numerical results

Figs. 1 and 2 shows the variation of the normalized real frequency (growth rate) $\omega_r/\omega_{pi}(\gamma/\omega_{pi})$ versus normalized wavenumber $(k\lambda_{dh})$ for different values of the wave propagation angle, θ shown on the curves. The parameters representative of auroral region, used here are, namely, normalized electron densities, $n_c/n_0 = 0.1, n_b/n_0 = 0.3, n_h/n_0 = 0.6$, hot to cold electron temperature ratio, $T_h/T_b = 50$, ratio of electron beam speed to hot electron thermal speed $U_b/v_{th} = 0.2$ and electron plasma to cyclotron frequency ratio, $\omega_{pe}/\omega_{ce} = 2$, respectively. It can be seen from these figures that as the angle of propagation increases, both real frequency and growth rate of the mode decreases for a fixed wavenumber. The corresponding range of wavelengths for which the mode can be excited also decreases. It implies that the waves propagating parallel to the magnetic field will have larger growth rate than the obliquely propagating waves. The waves propagating almost parallel to the ambient magnetic field are ion-acoustic like mode and the obliquely propagating waves are lower hybrid type of waves. It should be noted here that all the curves in this figure and subsequent figures are cutoff for the real frequency, $\omega_r \leqslant 0.3\omega_{ce}$ in order to satisfy the assumption for the low-frequency waves considered here.

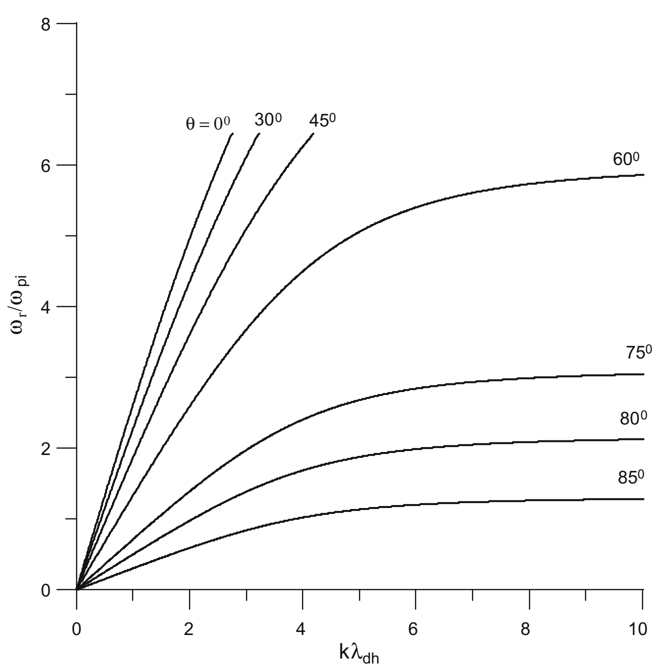

Fig. 1. Variation of the normalized real frequency, ω_r/ω_{pi} versus normalized wavenumber, $k\lambda_{dh}$ for different values of the wave propagation angle, θ as shown on the curves. Chosen parameters are: $n_c/n_0 = 0.1$, $n_b/n_0 = 0.3$, $n_h/n_0 = 0.6$, $T_h/T_b = 50$, $U_b/v_{th} = 0.2$ and $\omega_{pe}/\omega_{ce} = 2.0$.

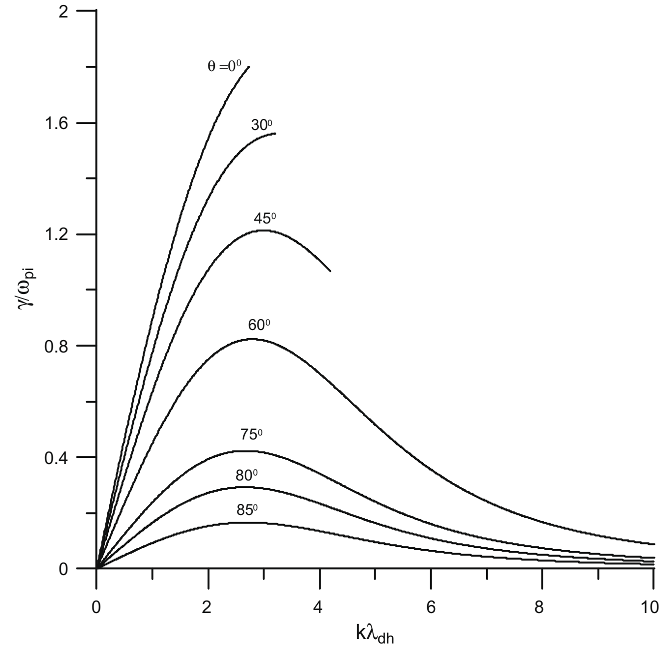

Fig. 2. Variation of the normalized growth rate, γ/ω_{pi} versus normalized wavenumber, $k\lambda_{dh}$ for different values of the wave propagation angle, θ as shown on the curves. Other parameters are same as for Fig. 1.

Fig. 3 shows the variation of normalized growth rate versus normalized wavenumber for different normalized electron beam speed, U_b/v_{th} as shown on the curves and $\theta = 30°$, for the parameters of Fig. 1. Numerical results show that the low-frequency waves can be excited for the $0.08 \leqslant U_b/v_{th} \leqslant 0.28$ for the set of parameters considered here.

Fig. 4 shows the variation of normalized growth rate versus normalized wavenumber for different values of ω_{pe}/ω_{ce} as shown on the curves and $\theta = 30°$. Other parameters are same as that of Fig. 1. It can be seen from the figure that as the ω_{pe}/ω_{ce} ratio increases the range of wavenumber for which the low-frequency mode can be excited decreases.

Fig. 5 shows the variation of normalized critical electron beam speed versus normalized wavenumber for different values of propagation angle θ as shown on the curves.

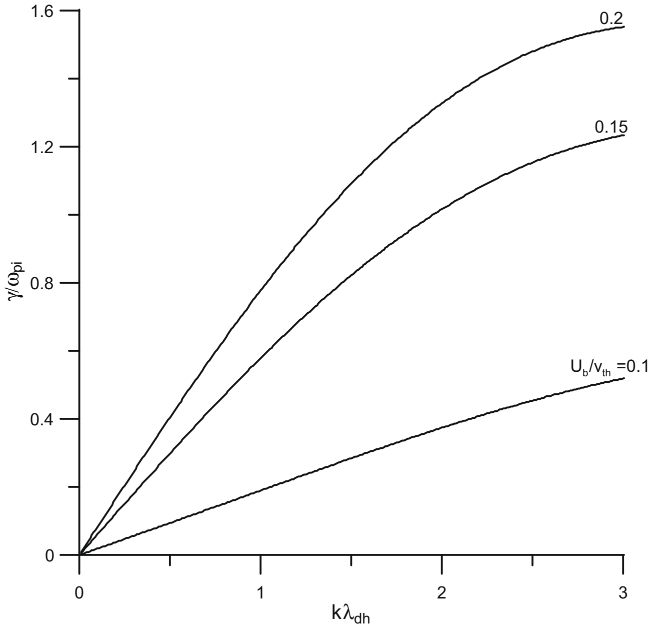

Fig. 3. Variation of the normalized growth rate, γ/ω_{pi} versus normalized wavenumber, $k\lambda_{dh}$ for different values of the U_b/v_{th} as shown on the curves and $\theta = 30^{\circ}$. Other parameters are same as for Fig. 1.

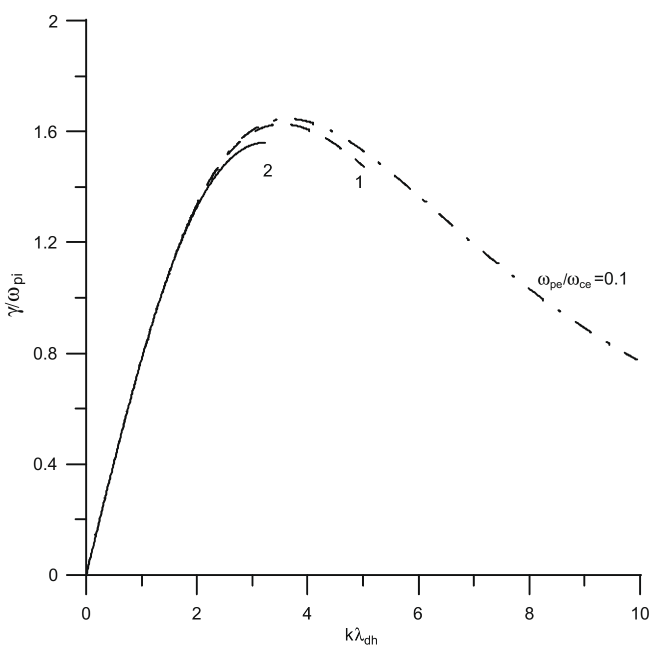

Fig. 4. Variation of the normalized growth rate, γ/ω_{pi} versus normalized wavenumber, $k\lambda_{dh}$ for different values of the ω_{pe}/ω_{ce} as shown on the curves and $\theta = 30°$. Other parameters are same as for Fig. 1.

Other parameters are same as that of Fig. 1. It can be seen from the figure that as the angle of propagation increases, the critical electron beam also increases, i.e., higher electron beam speed is required for more obliquely propagating waves.

Our numerical results also show that the growth rate decreases with the increase of cool and beam electron densities for other fixed parameters. The growth rate is very

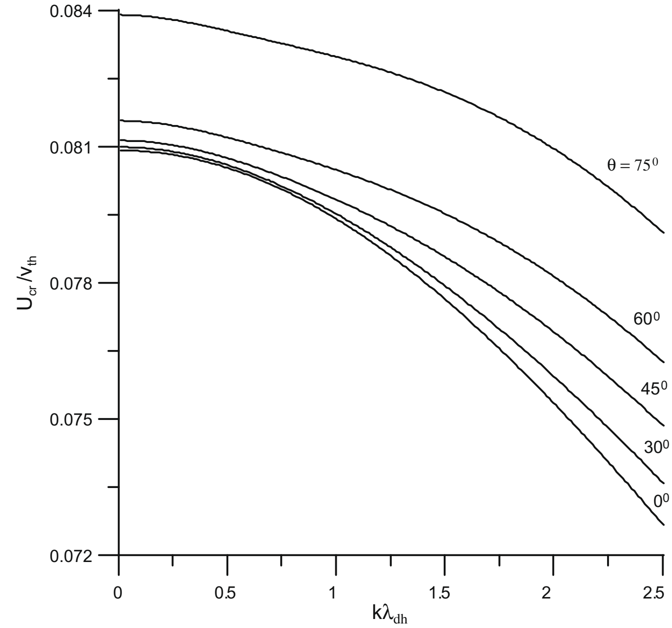

Fig. 5. Variation of the normalized critical beam speed U_{cr}/v_{th} versus normalized wavenumber, $k\lambda_{dh}$ for different values of the wave propagation angle, θ as shown on the curves. Other parameters are same as for Fig. 1.

sensitive to the angle of propagation. It is also seen that waves can not be excited for $T_h/T_b \geqslant 100$.

4. Conclusions

Tokar and Gary (1984) analyzed the full electromagnetic Vlasov dispersion equation and studied the stability of the electrostatic and electromagnetic waves for the case of upward moving electron beams observed in the polar cusp region. Their numerical simulations showed electron-acoustic waves (EAWs) to be unstable. Their model could explain the waves with frequencies below the electron plasma frequency. Singh and Lakhina (2001) studied the generation of electron-acoustic waves (EAWs) in an unmagnetized, four-component plasma consisting of stationary cold and hot Maxwellian electrons, drifting electron beam and ions. The results showed that waves with wide range of frequencies 5 Hz to 6 kHz can be excited through four-component model and can explain the broadband electrostatic noise (BEN) observations below the total electron plasma frequencies. The addition of hot background electrons to the previously existing three-component models of Gary and Tokar (1985) and Bharuthram (1991) reduces the excited EAW frequencies and growth rates. Recently, Sooklal and Mace (2004) showed that when plasma frequency of cool electrons exceed the electron gyro-frequency, at sufficiently large propagation angle, the electron-acoustic instability bifurcates into low-frequency electron-acoustic instability and higher frequency cyclotron sound instability. But their model has difficulties as while expanding the plasma dispersion function in the cool ion limit they have excluded the ion contribution to the real frequency, which is important while dealing with large angle of propagation (oblique propagation of waves in a magnetized plasma) around the lower hybrid frequencies or below. Further, they have assumed beam and warm electrons as unmagnetized that will demand very short perpendicular wavelengths and their model will be very restrictive to justify the assumptions. The dependence of real frequency and growth rate on the angle of propagation has not been described properly.

We have developed linear theory of low-frequency waves ($\omega << \omega_{ce}$) in a four-component magnetized plasma consisting of three types of electrons, namely cold background electron, warm electrons, warm electron beam and ions. All electron species are treated as magnetized as demanded by the low-frequency assumption (i.e., $\omega << \omega_{ce}$) for the waves.

For the parameters representative of auroral regions, namely, cold electron density, $n_c = 0.2\ \text{cm}^{-3}$, $n_h = 1.5\ \text{cm}^{-3}$, $n_b = 1\ \text{cm}^{-3}$, $T_b = 50$ eV, $T_h = 250$ eV (Dubouloz et al., 1991a,b, 1993), the real frequency and growth rate come out to be in the range of (17 Hz to 2.6 kHz) and 10 mHz to 60 Hz, respectively. The corresponding perpendicular wavelength of the mode is in the range of (1–70) km. It is interesting to note that the wave frequency calculated from our model for the low-frequency waves is well below the electron cyclotron, $f_{ce} = 7.4$ kHz and electron plasma, $f_{pe} = 14.8$ kHz frequencies. The cool electron plasma frequency is about 4 kHz. It can be seen that the waves which are well below the total electron plasma frequency can be explained through our model. The excited wave frequencies are also below the waves studied by Singh and Lakhina (2001) and Sooklal and Mace (2004).

Thus, our results can be applied to explain some features of the low-frequency part of the broadband electrostatic noise observed in the Earth's magnetosphere. Though, we have applied our results to the auroral region of the Earth's magnetosphere, however, they can be applied to other regions as well.

Acknowledgement

This work was done under the CAWSES-India project, "Boundary layer waves and ring current dynamics". S.V.S. and R.V.R. thank ISRO, Bangalore for financial support. G.S.L. thank the Council of Scientific and Industrial Research, Government of India, for the support under the Emeritus Scientist Scheme. S.V.S. would like to thank INSA, New Delhi for providing financial support for the COSPAR 2006 in Beijing, China.

References

Bharuthram, R. Electron-acoustic instability driven by a field-aligned hot electron beam. J. Plasma Phys. 46, 1–10, 1991.

Bostrom, R., Gustafsson, G., Holback, B., Holmgren, G., Koskinen, H., Kintner, P. Characteristics of solitary waves and weak double layers in the magnetospheric plasma. Phys. Rev. Lett. 61, 82–85, 1988.

Bounds, S.R., Pfaff, R.F., Knowlton, S.F., Mozer, F.S., Temerin, M.A., et al. Solitary potential structures associated with ion and electron beams near 1 R_E altitude. J. Geophys. Res. 104, 28709–28717, 1999.

Cattell, C., Dombeck, J., Wygant, J.R., Hudson, M.K., Mozer, F.S., et al. Comparisons of polar satellite observations of solitary wave velocities in the plasma sheet boundary and the high altitude cusp to those in the auroral zone. Geophys. Res. Lett. 26, 425–428, 1999.

Dubouloz, N., Pottellette, R., Malingre, M., Holmgren, G., Lindqvist, P.A. Detailed analysis of broadband electrostatic noise in the dayside auroral zone. J. Geophys. Res. 96, 3565–3579, 1991a.

Dubouloz, N., Pottelette, R., Malingre, M., Treumann, R.A. Generation of broadband electrostatic noise by electron acoustic solitons. Geophys. Res. Lett. 18, 155–158, 1991b.

Dubouloz, N., Treumann, R.A., Pottelette, R., Malingre, M. Turbulence generated by a gas of electron acoustic solitons. J. Geophys. Res. 98, 17415–17422, 1993.

Ergun, R.E., Calrson, C.W., McFadden, J.P., Mozer, F.S., Delory, G.T., et al. FAST satellite observations of large-amplitude solitary structures. Geophys. Res. Lett. 25, 2041–2044, 1998.

Franz, J.R., Kintner, P.M., Pickett, J.S. Polar observation of coherent electric field structures. Geophys. Res. Lett. 25, 1277–1280, 1998.

Gary, S.P., Tokar, R.L. The electron-acoustic mode. Phys. Fluids 28, 2439–2441, 1985.

Matsumoto, H., Kojima, H., Miyatake, T., Omura, Y., Okada, M., et al. Electrostatic solitary waves (ESW) in the magnetotail: BEN wave forms observed by GEOTAIL. Geophys. Res. Lett. 21, 2915–2918, 1994.

Mozer, F.S., Ergun, R.E., Temerin, M., Cattell, C., Dombeck, J., et al. New features of time domain electric field structures in the auroral acceleration region. Phys. Rev. Lett. 79, 1281–1284, 1997.

Omura, Y., Kojima, H., Matsumoto, H. Computer simulation of electrostatic solitary waves: a nonlinear model of broadband electrostatic noise. Geophys. Res. Lett. 21, 2923–2926, 1994.

Pottelette, R., Ergun, R., Treumann, R., Berthomier, M., Carlson, C., McFadden, J., Roth, I. Modulated electron-acoustic waves in auroral density cavities: FAST observations. Geophys. Res. Lett. 26, 2629–2632, 1999.

Roth, I., Hudson, M.K. Simulations of electron beam excited modes in the high-altitude magnetosphere. J. Geophys. Res. 91, 8001–8010, 1986.

Singh, S.V., Lakhina, G.S. Generation of electron-acoustic waves in the magnetosphere. Planet. Space Sci. 49, 107–114, 2001.

Sooklal, A., Mace, R.L. The magnetized electron-acoustic instability driven by a warm field-aligned electron beam. Phys. Plasmas 11, 1996–2008, 2004.

Temerin, M., Cerny, K., Lotko, W., Mozer, F.S. Observations of double layers and solitary waves in the auroral plasma. Phys. Rev. Lett. 48, 1175–1179, 1982.

Tokar, R.L., Gary, S.P. Electrostatic hiss and the beam driven electron acoustic instability in the dayside polar cusp. Geophys. Res. Lett. 11, 1180–1183, 1984.

Tsurutani, B., Arballo, J., Lakhina, G., Ho, C., Buti, B., Pickett, J., Gurnett, D. Plasma waves in the dayside polar cap boundary layer: bipolar, monopolar electric pulses and whistler mode waves. Geophys. Res. Lett. 25, 4117–4120, 1998.